Flood risk uncertainty surrounding a 0.5% annual probability event

J.M. Brown[1*], T. Prime[1,2], A.J. Plater[2]

[1] The National Oceanography Centre, Liverpool, L3 5DA, UK, *jebro@noc.ac.uk

[2] Liverpool University, Liverpool L69 3GP, UK

ABSTRACT

Ageing coastal defence is challenging managers to redesign schemes to be resilient, cost-effective and have minimal or beneficial environmental impact. To enable effective design, better understanding of the uncertainty in flood risk due to natural variability within the forcing is required. The typical UK design level is to withstand a 0.5% annual probability event, known historically as a 1 in 200 year return period event. However, joint wave-water level probability curves provide a range of conditions that meet this criterion. This is especially true in macrotidal regions with bi-modal wave climates. We take Dungeness and Rye Bay, a region of high value in terms of habitat and energy assets, as a case study that experiences such coastal conditions. This location has both natural defences, in the form of a gravel barrier, and engineered structures. Wave rider and tide gauge data are analysed to define joint probability curves. Points are taken along the 0.5% probability curve to form an ensemble of flood simulations to assess the uncertainty in impact of variable conditions that meet this classification. The wave events are first combined with the corresponding tide-surge elevations to calculate the spatial variability in tidally-varying wave overtopping along the defence frontage. This is used as boundary forcing to an inundation simulation. The uncertainty of the 0.5% probability flood hazard is examined to identify tipping points in the flood hazard, along with an assessment of which wave and water level combinations are most hazardous.

1. Introduction

Urbanisation, increasing sea-level and changes in storminess are all putting pressure on coastal systems (Hanley et al., 2014). The loss of natural environments and the need to protect communities is causing managers to rethink the design of coastal schemes (Bouma et al., 2015). To enable effective planning coastal monitoring is required to better understanding the local conditions and their interactions (Vugteveen et al., 2014), but also to capture information of extreme events and their frequency over long timescales (Wadey et al., 2015). In combination with observations, modelling studies are used to assess the uncertainty associated with the natural variability within the coastal forcing (Prime et al., submitted). UK flood management guidance is to use the joint probability of events occurring in combination (Hawkes, 2005), with typical flood defence levels designed to withstand a 0.5% annual probability event, known historically as a 1 in

200 year return period event (Environment Agency, 2015). However, joint wave-water level probability curves provide a range of conditions that meet this criterion. This is especially true in macrotidal regions with bi-modal (swell and locally generated) and bi-directional wave climates. We take Dungeness and Rye Bay, a region of high value in terms of habitat and energy assets, as a case study that experiences such coastal conditions (Idier et al., 2012; Mason et al., 2008). By addressing the uncertainty in the flood hazard generated by the range of events considered as having a 0.5% probability of occurrence we can identify the water-wave combinations that pose greatest threat for the purpose of flood management.

The case study site is presented in Section 2, followed by a description of the numerical methods in Section 3. The results are presented in Section 4 before a discussion in Section 5 and concluding remarks in Section 6.

2. Study Site

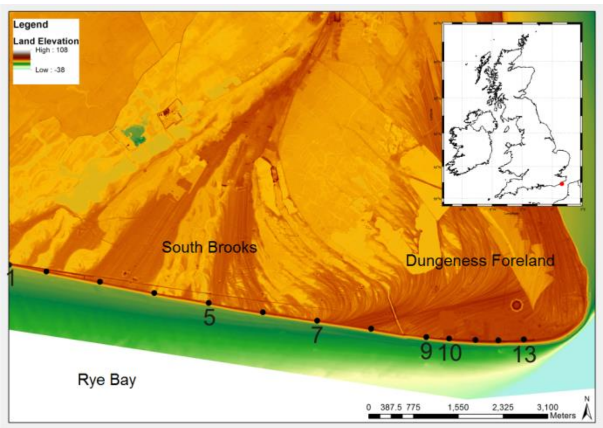

FIG. 1. The model domain covering Rye Bay and Dungeness Foreland. The black dots denote the location of the beach profiles in Fig. 2.

Rye Bay and Dungeness Foreland are located in the southeast of the UK, within the English Channel (Fig. 1). We focus on the southern shoreline of the Dungeness Foreland facing Rye Bay. The area is considered energetic due to its position at the downwind end of one of the stormiest seas in the UK – the English Channel (Long et al., 2006). The wave climate is bi-modal in the fact it receives both swell and locally generated waves (Mason et al., 2008), while also being bi-directional, with waves coming from the southwest and northeast – the largest from the southwest. The tides are considered macrotidal, with a semi-diurnal tidal range of approximately 6.7 m in Rye Bay (Stupples, 2002). The skew surge in this region, known as the Dover Straight, can reach several tens of centimetres (Idier et al., 2012). This location has both natural defences, in the form of a gravel barrier, and engineered structures (Fig. 2). Beach survey data from August 2014 are used to assess the resilience of this shoreline to an event with 0.5% probability of occurrence. Moving from west to east along the frontage the subtidal profiles become deeper. The profiles 1-9 (located in Fig. 1) represent the natural barrier of variable crest level and width, lower crest levels occur at profile 5 and 7 (blue profiles, Fig. 2), while the other profiles have similar elevation (green profiles, Fig. 2). Behind the gravel barrier (profiles 2-7, Fig. 1) there is a natural embankment creating a secondary defence for the low-lying marshland – known locally as the “green wall”. At the eastern end the natural barrier is backed by a seawall, profiles 10-13, creating a much higher and steeper crest profile (red profiles, Fig.2).

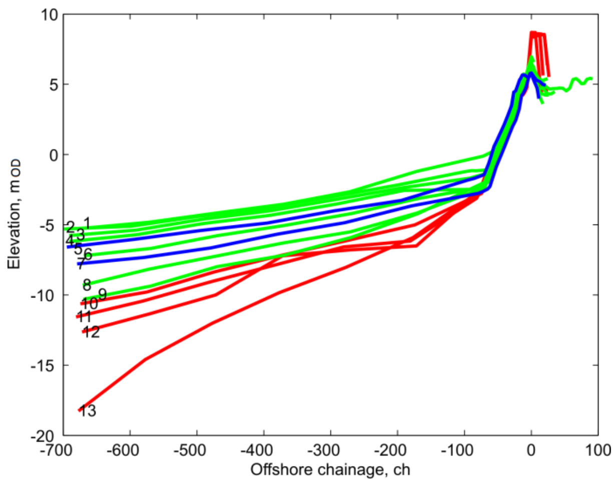

FIG. 2. Beach survey profiles (located in Fig. 1) of the engineered (red) and natural (green and blue) system. The blue profiles depicting lower barrier heights.

Although the southern shore has a natural resilience to flood risk it is considered vulnerable due to the future availability of sediment and changes in sea level and storm conditions (Plater et al., 2009). Better understanding of the uncertainty in local flood hazard is critical for managing human intervention within the designated Site of Special Scientific Interest (SSSI), and to ensure a resilient energy supply. The site in question is designated as a SSSI for both biological and geological/geomorphological significance and the energy installation has been granted a 10-year extension to its operational cycle beyond 2018.

To inform managers of the uncertainty in the flood hazard generated by a specified return level we base this study on easily accessible nearby observations from the Hastings wave rider (50° 44.79´N, 0° 45.30´E) and the Dover tide gauge (51° 6.86´N, 1° 19.35´E). The wave data are collected by WaveNet, a UK wave rider network maintained by CEFAS, and are available from November 2006. The water levels have been recorded more consistently since 1958 as part of the NTSLF tide gauge network delivered through the BODC.

3. Method

We focus on classifying the uncertainty in flood depths and extent generated by a 0.5% probability event. The full details are available in Prime et al. (submitted). Wave rider and tide gauge data are analysed to define joint probability curves (Fig. 3). The data for every available high water event with associated wave condition at that time is processed by the JOIN-SEA software (Hawkes and Gouldby, 1998) to calculate the probability curves of occurrence. The short duration of the wave data limits the analysis to high water events in the period 26/11/2002 to 28/07/2014. Using the JOIN-SEA software (Hawkes et al., 2002) 30 points are taken along the 0.5% probability curve to form an ensemble of flood simulations to assess the uncertainty in the impact of variable conditions that meet this event classification. These scenario events represent the section of the curve where there is most variation in the joint conditions. They include observed high water levels varying from 1.2 – 4.6 m ODN and significant wave heights varying from 1.6 – 4.7 m. The majority of the waves have a peak period of 10 s, but range from 8.3 s to 16.7 s. The events are first used in an XBeach-G simulation to calculate the spatial variability in tidally-varying wave overwashing along the defence frontage. These are then applied as boundary forcing to a LISFLOOD-FP inundation simulation.

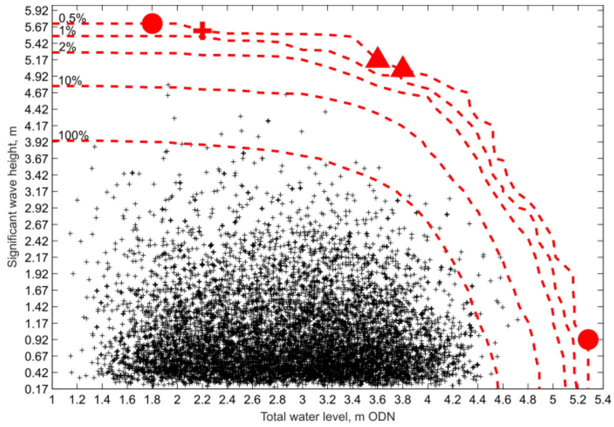

FIG. 3. Joint probability curves. The red circles bound the section used in the uncertainty analysis, the red cross marks the tipping point when wave-water level conditions enable the overwashing of defences, and the red triangles identify a second tipping point regime in the extremity of the flood hazard.

XBeach-G (McCall et al., 2015) is applied to the 13 beach profiles (Fig.2) to simulate both the overwashing and evolution of the gravel-engineered frontage. The 1D simulations have a 1 m cross-shore resolution and are spaced at 1 km intervals along the natural barrier (locations 1-9, Fig. 1) and at 500 m intervals where additional engineered intervention is imposed around the energy installation (locations 10-13, Fig. 1). A mean spring tide is combined with a statistically derived surge curve (McMillan et al., 2011) to achieve the extreme water levels for the conditions representing a 0.5% probability event. The synthetic storm tide is applied with the corresponding wave level for each scenario in XBeach-G. A linear relation between the wave heights and peak periods is used to obtain the highest energy wave condition representative of each scenario. Over the storm tide cycle the wave input (height and period) is kept constant, although variability in the wave field is accounted for through the use of a JONSWAP spectrum in XBeach-G. This approach enables the worst case scenario to be simulated as the wave conditions are maintained for the full duration of the simulation. The overwashing discharge for the duration of the storm tide is obtained at the defence crest level, defined by the final beach profile during the morphological simulation.

LISFLOOD-FP (Bates and De Roo, 2000) is used to simulate the inundation due to the overwashing conditions. The model domain (Fig. 1) is set up at 5 m resolution using a composite of LiDAR data from 2009 provided by the EA. The coastal boundary is imposed as the defence crest level along which the overwashing time-series data are imposed. From LISFLOOD-FP the flood hazard is provided in addition to the flood inundation.

The uncertainty of the 0.5% probability flood hazard is examined using the ensemble of simulations. For each event the 95th percentile of the time-varying overwashing discharge is calculated, along with the number of profiles that overwashed, and the 50th percentile of the spatial variability in the maximum flood hazard value during the duration of the scenario over the inundated area. The hazard values are rated as very low danger if ≤ 0.75; a danger to some (elderly and children) if ≤ 1.25 and > 0.75; a danger to most (general public) if ≤ 2.00 and > 1.25; or a danger to all (including emergency services) if > 2.0. This 50th percentile rating therefore does not include the small areas of the much deeper flood water, but the more median flood depths experienced across the flood plain. The higher 95th percentile value is used for the overwashing to capture the more extreme rates around high water during the period of the event in this analysis.

4. Results

The coastal conditions are analysed relative to the flood hazard caused over 50% of the inundated region. An assessment of which wave and water levels generate the most extreme conditions for marine inundation is presented first (Fig. 4). It is clear that there is a linear relation between the increase in extreme water level and the increase in the hazard, while the relation between the wave heights and hazard is related with an inversely exponential trend. The largest hazard is associated with the highest water levels and lowest (long period) swell waves. A clear, but sudden, change in the hazard value from 0.5 to 1 is seen in the scenarios. The shaded area in Fig. 4 represents the region of uncertainty around the exact wave-water level combinations that cause the tipping point in hazard value.

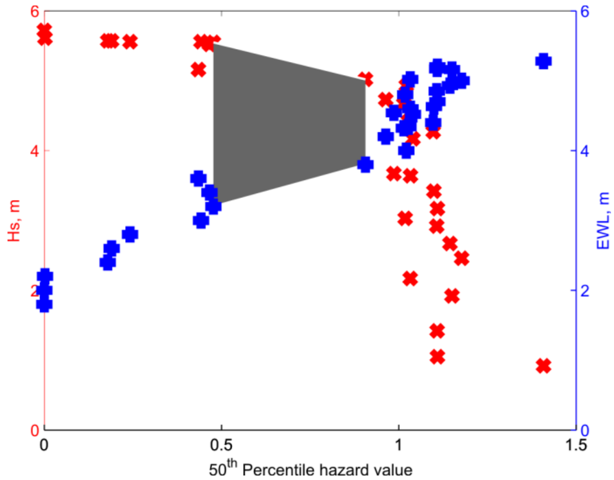

FIG. 4. The extreme water level (EWL in blue) and significant wave height (Hs in red) for each of the 30 simulated events is plotted verses the hazard value of the scenarios. The shaded area represents the region of uncertainty associated with the combined wave-water level conditions that cause a tipping point in the hazard value.

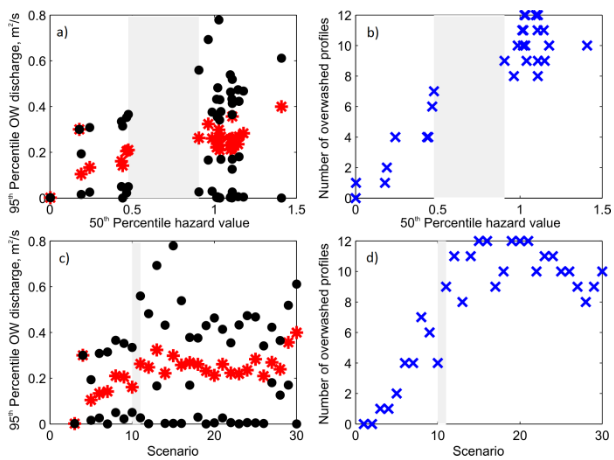

FIG. 5. The maximum (upper black dots), minimum (lower black dots) and mean (red stars) overwashing (OW) discharge for the 13 profiles during each

simulation (left column), and number of overwashed profiles during each simulation (right column) in relation to the hazard value (top row) and the order of the 30 scenario events (bottom row) between the circles in Fig. 3. The shaded area positions the tipping point in the hazard value seen in Fig. 4.

The overwash discharge (Fig. 5a) indicates an increase in the maximum 95th percentile overwashing discharge occurs after the tipping point in increased hazard. This is also seen in the mean and minimum overwash values, but to a lesser extent. There is a fairly linear trend in the number of profiles experiencing overwashing and the hazard value (Fig. 5b), with consistently more profiles being overtopped after the tipping point in the hazard value. However, when compared with the scenarios in order as they occur along the probability curve (Fig. 3), these trends diminish. The maximum overwashing rates clearly occur soon after the tipping point in the hazard value, but then revert to lower rates with decreasing wave height (Fig. 5c). The number of overwashed profiles continues to steadily increase with increased water levels and then tails off with lowering wave heights (Fig. 5d). Although, an increase is again seen for the last few events when the wave period starts to noticeably increase and has a more dominant impact.

Next we show the flood depth and extent for the events that cause a tipping point in the hazard generated from wave overwashing. No overwashing occurs until the water level reaches 2.2 m, enabling 5.6 m, 10 s waves to overwash the low points in the primary defences (located on the probability curve by a cross in Fig. 3). The overwashing initially starts as a fan around profile 7 (e.g. Fig. 6a). With increasing water levels the number of overwashing fans spreads along the frontage, but the majority of the water is contained by the secondary defence (e.g. Fig. 6b). Water levels increasing from 3.6 m and 3.8 m with waves decreasing from 5.16 m to 5.02 m in height increases the number of overwashing profiles and the overwash rate, enabling water to spill over the secondary defence, causing a tipping point in the inundation extent and depth (e.g. Fig. 6c). This state change in inundation is what causes the tipping point in the hazard rating. Fig. 6 clearly suggests a large uncertainty envelope is associated with the inundation map of a 0.5% probability flood event at this location. For the full range in possible flood extents for this model application see Prime et al. (submitted).

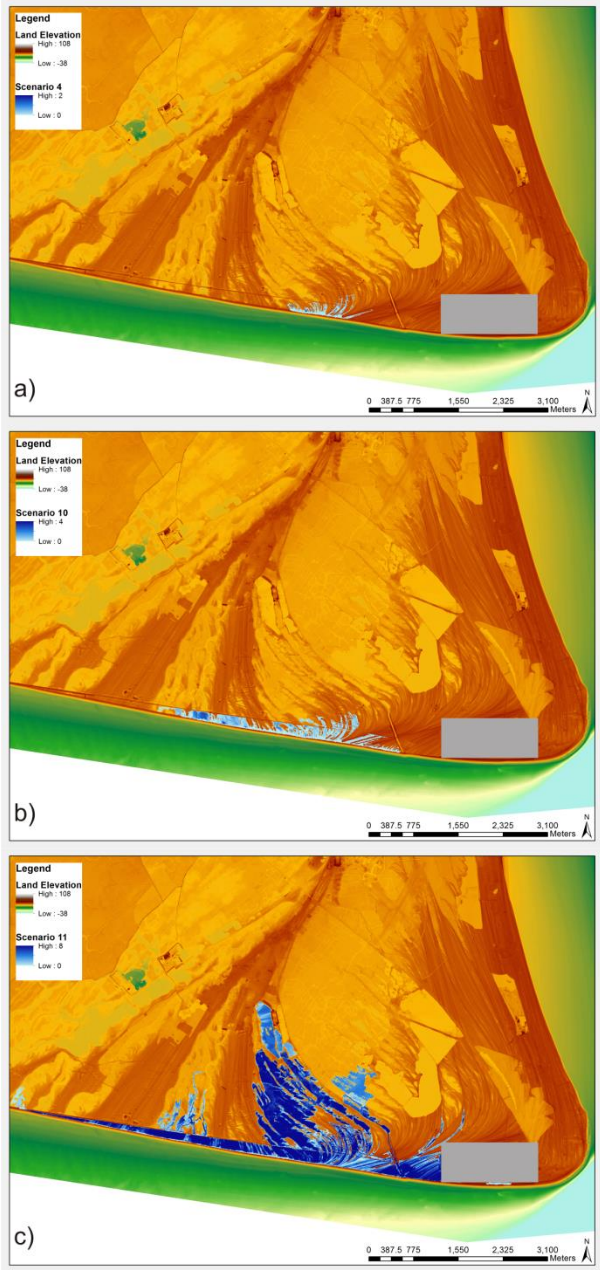

FIG. 6. The flood inundation for (a) scenario 4, just after the onset for flooding scenario 3 (Fig. 3), (b) scenario 10 just before the tipping point in the flood hazard (Fig. 3), and (c) scenario 11 just after the tipping point in the flood hazard (Fig. 3). The grey shading delimits the energy assets where management interventions are outside the scope of this study.

5. Discussion

This analysis is limited by the short data length of the wave record, which reduces the accuracy of the low probability 0.5% occurrence events. However, the curve can still be used to assess the uncertainty in the flood hazard and identify events that cause a tipping point in the overwash conditions and/or the flood extent. For all events the hazard value is below 1.5. For a 0.5% probability event there is potentially a risk to the general public during this event if associated with high water level and low wave height conditions associated with this event classification. Since the hazard rating is defined as the 50th percentile maximum hazard value the higher risk areas also make up 50% of the inundated area. We show that the hazard rating is related to extreme water level, which in turn control the rate and number of overwashing events within a scenario. The highest number of overwashing profiles and the highest rates of overwashing are associated with scenarios of high hazard value relative to the tipping point. However, the maximum hazard rating is not associated with the highest values in either property. On close inspection a second tipping point between a hazard value of 1.2 and 1.4 also occurs. This could be associated with a change in the wave period. The greatest hazard being associated with the only 16.7 s wave condition, the periods associated to other high hazard values are lower between 10 and 13.3 s.

With increasing water levels the overwashing rate has a greater range in variability along the frontage. The number of overwashing profiles increases until a point is reached when the decreasing wave height counteracts the increasing water level and the number of overwash locations reduces. The later scenarios with increasing wave periods again allow an increase in the number of overwash locations. Since the flood hazard does not show this trend the decreasing number of profiles providing a source of flood water must be counteracted with a generally higher discharge. It is seen that after the tipping point in the hazard value the mean discharge is generally similar at a consistently high levels for all scenarios, while the maximum value is more variable.

6. Conclusion

By calculating the flood hazard for a range of wave-water level conditions, which are all classified the as the same extreme event – a 0.5% probability event – we show that there is a great uncertainty in the flood hazard. Higher water levels enable greater wave overwashing, which counteracts any influence of a decreasing wave height. The longest period low swell waves combined with the highest extreme water levels cause the greatest hazard.

Tipping points within the flood hazard from wave overwashing are associated with the terrain of the location, with water being constrained by a natural secondary defence. It is also suggested that a second trigger in increased flood hazard occurs in response to the wave period. This study suggests it is the high water, low wave region of the probability curve that needs to be considered when designing the next generation of coastal schemes to withstand a specified return level in extreme events.

Acknowledgments

This research was funded through the ERIIP “Sandscaping for Mitigating Coastal Flood and Erosion Risk to Energy Infrastructure on Gravel Shorelines: a case study approach” project (NERC NE/M008061/1), the ARCC “Adaptation and Resilience of Coastal Energy Supply” (ARCoES) project (EPSRC EP/I035390/1), and the Multi-Event Modelling Of Risk and recovery project (FloodMEMORY) funded (EP/K013513/1). The Crown Estate and Tom Dauben at the EA are thanked for their contributions to this research. The Channel Coastal Observatory, the EA, CEFAS and, NTSLF, BODC are thanked for the provision of beach survey, LiDAR, WaveNet wave rider and UK tide gauge data at the study site.

REFERENCES

Bates P.D., De Roo A.P.J. (2000) A simple raster-based model for flood inundation simulation. J Hydrol., 236: 54–77.

Bouma, T.J., van Belzen, J., Balke, T., Zhu, Z., Airoldi, L., Blight, A.J., Davies, A.J., Galvan, C., Hawkins, S.J., Hoggart, S.P.G., Lara, J.L., Losada, I.J., Maza, M., Ondiviela, B., Skov, M.W., Strain, E.M., Thompson, R.C., Yang, S., Zanuttigh, B., Zhang, L., Herman, P.M.J. (2014) Identifying knowledge gaps hampering application of intertidal habitats in coastal protection: Opportunities & steps to take. *Coastal Engineering*, 87: 147-157.

Environment Agency (2015), Flood Map - your questions answered, U. K. Available from: http://apps.environment-agency.gov.uk/wiyby/31662.aspx (Accessed 11 March 2015)

Hawkes P.J. (2005). Use of joint probability methods in flood management: A guide to best practice. Defra / Environment Agency R&D Technical Report FD2308/TR2,

Hanley, M.E., Hoggart, S.P.G., Simmonds, D.J., Bichot, A., Colangelo, M.A., Bozzeda, F., Heurtefeux, H., Ondiviela, B., Ostrowski, R., Recio, M., Trude, R., Zawadzka-Kahlau, E., Thompson, R.C. (2014) Shifting sands? Coastal protection by sand banks, beaches and dunes, *Coastal Engineering*, 87: 136-146.

Hawkes, P., Gouldby, B. (1998) The joint probability of waves and water levels: JOINSEA-User Manual, HR Wallingford, Wallingford, UK.

Hawkes, P.J., Gouldby, B.P., Tawn, J.A., Owen, M.W. (2002) The joint probability of waves and water levels in coastal engineering design, J. Hydraul. Res., 40, 241–251.

Idier, D., Dumas, F., Muller, H. (2012) Tide-surge interaction in the English Channel. Nat. Hazards Earth Syst. Sci., 12(12): 3709-3718.

Long, A.J., Waller, M.P., Plater, A.J. (2006) Coastal resilience and late Holocene tidal inlet history: The evolution of Dungeness Foreland and the Romney Marsh depositional complex (U.K.), *Geomorphology*, 82(3–4):309-330.

Mason, T., Bradbury, A., Poate, T. and Newman, R. (2009) Nearshore wave climate of the English Channel - evidence for bi-modal seas. In, Coastal Engineering 2008. 31st International Conference on Coastal Engineering New York, USA, American Society of Civil Engineers, 605-616.

McCall, R.T., Masselink, G., Poate, T.G., Roelvink, J.A., Almeida, L.P. (2015) Modelling the morphodynamics of gravel beaches during storms with XBeach-G, *Coastal Engineering*, 103: 52-66.

McMillan A, Batstone C, Worth D, Tawn J, Horsburgh K, Lawless M. (2011) Coastal flood boundary conditions for UK mainland and islands. Project SC060064/TR2: Design sea levels.

Plater, A.J., Stupples, P., Roberts, H.M., (2009) Evidence of episodic coastal change during the Late Holocene: The Dungeness barrier complex, SE England, *Geomorphology*, 104(1–2): 47-58.

Prime, T., Brown, J.M., Plater, A.J. (submitted) Flood inundation uncertainty: the case of a 0.5% probability flood event, Environmental Science & Policy.

Stupples, P. (2002) Tidal cycles preserved in late Holocene tidal rhythmites, the Wainway Channel, Romney Marsh, southeast England, *Marine Geology*, 182(3–4): 231-246.

Vugteveen, P., van Katwijk, M.M., Rouwette, E., Hanssen, L. (2014) How to structure and prioritize information needs in support of monitoring design for Integrated Coastal Management, Journal of Sea Research, 86: 23-33.

Wadey, M.P., Brown, J.M., Haigh, I.D., Dolphin, T., Wisse, P. (2015) Assessment and comparison of extreme sea levels and waves during the 2013/2014 storm season in two UK coastal regions, Hazards Earth Syst. Sci., 15(10): 2209-2225.